

Article

Acid-Mediated Migration of Bromide in an Antiaromatic Porphyrinoid: Preparation of Two Regioisomeric Ni(II) Bromonocorroles

Hiroyuki Kawashima, Satoru Hiroto, and Hiroshi Shinokubo

J. Org. Chem., **Just Accepted Manuscript** • DOI: 10.1021/acs.joc.7b01899 • Publication Date (Web): 13 Sep 2017

Downloaded from <http://pubs.acs.org> on September 14, 2017

Just Accepted

“Just Accepted” manuscripts have been peer-reviewed and accepted for publication. They are posted online prior to technical editing, formatting for publication and author proofing. The American Chemical Society provides “Just Accepted” as a free service to the research community to expedite the dissemination of scientific material as soon as possible after acceptance. “Just Accepted” manuscripts appear in full in PDF format accompanied by an HTML abstract. “Just Accepted” manuscripts have been fully peer reviewed, but should not be considered the official version of record. They are accessible to all readers and citable by the Digital Object Identifier (DOI®). “Just Accepted” is an optional service offered to authors. Therefore, the “Just Accepted” Web site may not include all articles that will be published in the journal. After a manuscript is technically edited and formatted, it will be removed from the “Just Accepted” Web site and published as an ASAP article. Note that technical editing may introduce minor changes to the manuscript text and/or graphics which could affect content, and all legal disclaimers and ethical guidelines that apply to the journal pertain. ACS cannot be held responsible for errors or consequences arising from the use of information contained in these “Just Accepted” manuscripts.

1
2
3
4
5
6
7
8
9
10
11
12
13
14
15
16
17
18
19
20
21
22
23
24
25
26
27
28
29
30
31
32
33
34
35
36
37
38
39
40
41
42
43
44
45
46
47
48
49
50
51
52
53
54
55
56
57
58
59
60

Acid-Mediated Migration of Bromide in an Antiaromatic Porphyrinoid: Preparation of Two Regioisomeric Ni(II) Bromonorcorroles

*Hiroyuki Kawashima, Satoru Hiroto, and Hiroshi Shinokubo**

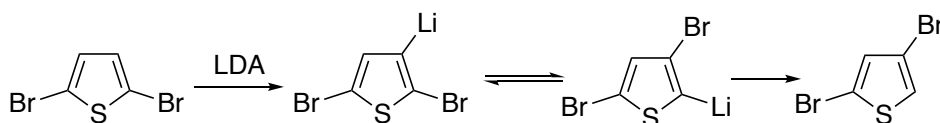
Department of Molecular and Macromolecular Chemistry, Graduate School of Engineering,
Nagoya University, Furo-cho, Chikusa-ku, Nagoya 464-8603, Japan

ABSTRACT: Regioselective halogenation of porphyrinoids is critical for their selective functionalization, which enables fine-tuning of their electronic and optical properties. Here we report the synthesis of two regioisomeric Ni(II) bromonorcorroles on the basis of acid-induced migration of the bromo substituent. Treatment of Ni(II) dimesitylnorcorrole with *N*-bromosuccinimide (NBS) selectively afforded Ni(II) 3-bromonorcorrole, which was further converted into Ni(II) 2-bromonorcorrole upon treatment with hydrogen bromide. In addition, the reaction of Ni(II) dimesitylnorcorrole with an excess amount of NBS afforded the octabrominated product. The reaction mechanism of the bromination reaction of Ni(II) dimesitylnorcorrole was investigated by theoretical calculations.

Introduction

A halogen dance reaction of halogenated aromatic compounds is a powerful methodology to effectively expand the diversity of aryl halides, thus enabling a variety of regioselective functionalizations of aromatic compounds (Scheme 1).¹ Generally, the halogen dance reaction occurs under basic conditions involving migration of the halogen atom to a highly reactive anionic carbon center via a lithium–halogen exchange reaction. In contrast, rearrangement of a halogen atom has been rarely observed under acidic conditions and regioselective halogen migration has not been well documented.²

Scheme 1. A representative halogen dance reaction of 2,5-dibromothiophene.



Peripheral functionalization of porphyrins is essential to modulate their electronic and photophysical properties.³ To achieve site-specific functionalization of porphyrins, a halogen substituent at the porphyrin periphery is often employed as a foothold to introduce various functionalities at the desirable position of porphyrins. Consequently, regioselective halogenation of porphyrins has been extensively investigated.⁴ However, the regioselectivity in electrophilic halogenation of porphyrins is determined by the electron density of the peripheral positions. It is difficult to override the inherent selectivity by other factors. In addition, porphyrinoids have many similar reactive sites on the pyrrole subunits. It is generally difficult to prepare different types of halogenated products regioselectively depending on the reaction conditions.

Norcorrole is a ring-contracted porphyrin with a 16π -antiaromatic conjugation system, which lacks two *meso*-carbons from a regular porphyrin.^{5,6} Recently, we have synthesized an

1
2
3 antiaromatic Ni(II) norcorrole complex **1**.⁷ The reactivity of **1** has been explored in several types
4
5 of reactions such as oxidation, reduction, nucleophilic substitution, and silylene-insertion.⁸
6
7
8 Recently, Li, Chmielewski, and co-workers have also reported intriguing reactions of **1** with
9
10 several reagents.⁹
11

12 Here we wish to disclose a method to prepare two regioisomeric brominated norcorrole Ni(II)
13
14 complexes selectively depending on the reaction conditions. We have found that electrophilic
15
16 brominating reagents delivered a bromine atom selectively at the C3 position of Ni(II)
17
18 dimesitylnorcorrole **1**. Interestingly, Ni(II) 3-bromonorcorrole selectively rearranged into 2-
19
20 bromonorcorrole under acidic conditions. These two bromonorcorroles were transformed to
21
22 functionalized norcorroles through cross-coupling reactions, which elucidate the substituent
23
24 effect at the 2- and 3-positions to the antiaromatic 16 π -electronic system. In addition, treatment
25
26 of **1** with an excess amount of *N*-bromosuccinimide (NBS) resulted in formation of
27
28 octabrominated product, which was transformed through Migita–Kosugi–Stille coupling to Ni(II)
29
30 octaalkynylnorcorrole with substantially enhanced near IR absorption property.
31
32
33
34
35
36
37
38

39 **Results and Discussion**

40 **Bromination of Ni(II) dimesitylnorcorrole**

41
42 Bromination of Ni(II) dimesitylnorcorrole **1** with several electrophilic brominating reagents
43
44 was investigated. We found that treatment of **1** with 1.1 equiv of NBS in THF at –60 °C
45
46 furnished 3-brominated product **2a** in 72% yield regioselectively (Scheme 2). None of other
47
48 isomeric bromonorcorroles was detected in the reaction mixture. The regioselectivity for 3-
49
50 substituted norcorrole is the same as that observed in nitration of **1**, reported by Li and
51
52 Chmielewski.^{9a} Compound **2a** was fully characterized by its NMR and MS analysis. The
53
54
55
56
57
58
59
60

position of the bromine atom in **2a** was unambiguously determined by the X-ray diffraction analysis (Figure 1a and Figure S20). The use of *N*-bromophthalimide (NBP) also afforded **2a** in a comparable yield (69% yield). The use of bromine and bis(*sym*-collidine)bromide hexafluorophosphate¹⁰ as brominating reagents at $-60\text{ }^{\circ}\text{C}$ also exhibited the same regioselectivity to furnish only **2a** in 53% and 61% yields, respectively.

Scheme 2. Bromination of norcorrole **1** with NBS and bromine.

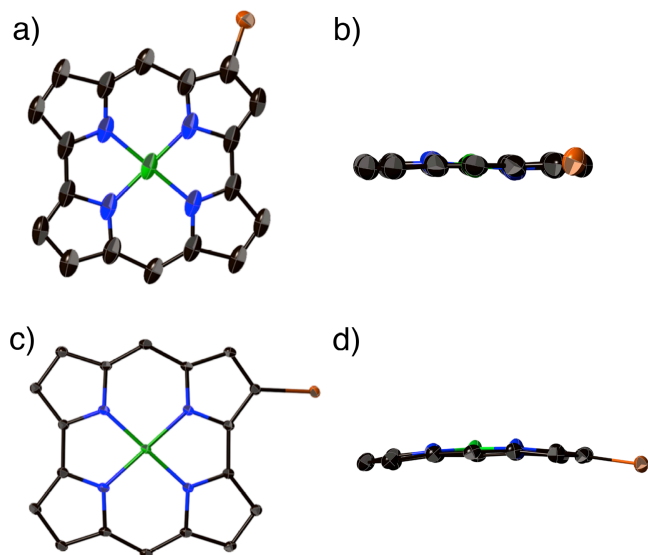
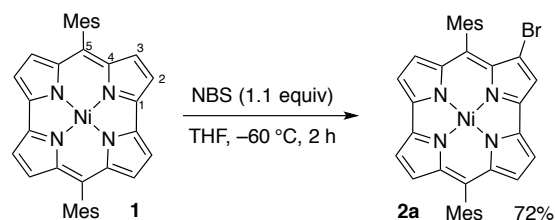
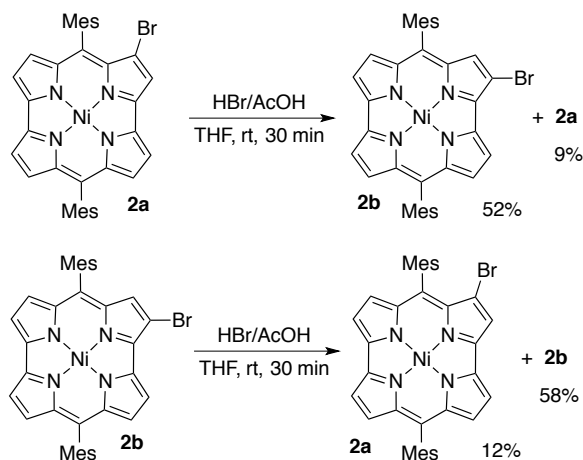


Figure 1. X-Ray crystal structures of **2a** and **2b**. a) Top and b) side views of **2a** and c) top and d) side views of **2b**. Atomic displacement parameters are set at 50% probability and mesityl groups are omitted for clarity.

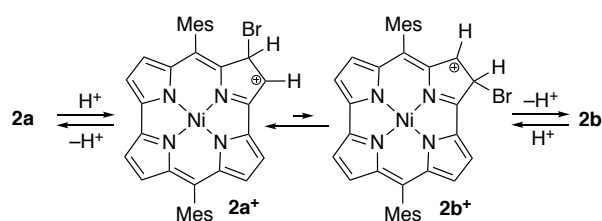
Interestingly, 2-brominated product **2b** was selectively obtained in 27% yield with bromine at room temperature. The slightly domed structure of **2b** was elucidated by single crystal X-ray

1
2
3 analysis (Figure 1c and Figure S21). Unfortunately, however, the reaction with bromine lacked
4
5 in reproducibility, and the observed regioselectivity for **2a** vs. **2b** was sensitive to the reaction
6
7 conditions such as reaction temperatures and the workup procedures.
8
9

10 It prompted us to examine the reaction conditions to understand the key factor for the
11
12 ambiguous selectivity for **2b**. While the bromination reaction with NBS is almost neutral,
13
14 hydrogen bromide should be formed as a byproduct in the reaction with Br₂. We eventually
15
16 revealed that hydrogen bromide was essential for the formation of **2b** (Scheme 3). In fact,
17
18 treatment of **2a** with an excess amount of hydrogen bromide in THF at room temperature
19
20 induced migration of the 3-bromo group to the 2-position, furnishing 2-brominated product **2b** in
21
22 52% yield along with recovery of **2a** in 9% yield. Importantly, migration of the bromine atom is
23
24 reversible at room temperature: The reaction of **2a** with HBr under the same reaction conditions
25
26 provided **2a** and **2b** in 58% and 12% yields, respectively, along with **1** in 15% yield. These
27
28 results indicate the existence of equilibrium between **2a** and **2b** under acidic conditions at room
29
30 temperature. In addition, partial debromination also occurred under these conditions.
31
32
33
34
35
36
37
38
39
40
41
42
43
44
45
46
47
48
49
50
51
52
53
54
55
56
57
58
59
60

Scheme 3. Rearrangement of bromonorcorroles **2a** and **2b**.**Reaction mechanism of bromination of Ni(II) norcorrole**

Li, Chmielewski, and co-workers have investigated the origin of the 3-position selectivity in nitration of **1** on the basis of the density functional theory (DFT) calculations.^{9a} They concluded that the stability of arenium type cation intermediates is essential in determining the major nitration product. In the case of bromination of **1**, we also consider the relative stability of brominated arenium cations governs the regioselectivity for 3-brominated norcorrole **2a**. Then, the issue is the reason for the 2-position selectivity in the reaction of **2a** with HBr to form **2b**.

Scheme 4. Proposed reaction mechanism for bromine migration.

Because bromination of **1** with either NBS or Br₂ selectively afforded the same product **2a** at low temperatures, the key factor should be the reaction temperature and the amount of hydrogen bromide in the reaction mixture. On the basis of the finding that the HBr-induced migration

1
2
3 reaction is reversible, we propose the following reaction mechanism (Scheme 4). Protonation of
4
5 **2a** with HBr provides cationic intermediate **2a⁺**, which is in equilibrium with **2b⁺**. Deprotonation
6
7 of cationic intermediate **2b⁺** yields **2b** as a more stable product. At low temperatures under
8
9 neutral conditions, the reaction selectively furnished **2a**, indicating that **2a** is a kinetically
10
11 favorable product. In contrast, **2b** is thermodynamically more stable due to its less sterically
12
13 demanding nature.
14
15

16
17 To verify the proposed mechanism, we conducted DFT calculations on the reaction products,
18
19 arenium cation intermediates, and transition states at the B3LYP/6-31+G(d,p)+SDD level
20
21 (Figure S24 and Table S1).^{11,12} The solvent effect of THF was considered with the polarizable
22
23 continuum model (PCM) method.¹³ The cationic intermediate **2a⁺** is more stable by 1.27 kcal
24
25 mol⁻¹ than **2b⁺** (Figure 2a). The origin of the relative stability of **2a⁺** over **2b⁺** is not clear at this
26
27 moment but we now speculate that the cationic charge is more effectively delocalized in **2a⁺** than
28
29 in **2b⁺** as indicated in the resonance structures of **2a⁺** over **2b⁺** (Figure S29 and S30). For the
30
31 migration process between **2a⁺** and **2b⁺**, a three-membered ring bromonium species **TS1** was
32
33 located as a transition state. The activation barrier from **2a⁺** to **2b⁺** via **TS1** is 24.4 kcal mol⁻¹.
34
35 The deprotonation processes from the cationic intermediates **2a⁺** and **2b⁺** with a bromide anion
36
37 were also calculated and transition states **TS2** and **TS3** were found, respectively. The activation
38
39 energies for deprotonation of **2a⁺** and **2b⁺** are 5.8 and 3.6 kcal mol⁻¹, respectively (Figure 2b,c).
40
41 Considering the substantially higher activation barrier of the migration process, the bromination
42
43 reaction and the subsequent deprotonation at low temperatures should occur under kinetic control,
44
45 yielding 3-brominated product **2a** through more stable intermediate **2a⁺**. On the other hand,
46
47 protonation processes of **2a** and **2b** require 8.6 and 8.0 kcal mol⁻¹ of activation energies,
48
49 respectively. This result indicates that re-protonation of **2a** and **2b** is facile at high temperatures
50
51
52
53
54
55
56
57
58
59
60

1
2
3 under highly acidic conditions in the presence of an excess amount of HBr. In this situation, the
4
5 whole processes are reversible at high temperatures, favoring the formation of more
6
7 thermodynamically stable **2b**, which is thermodynamically more stable by 3.6 kcal mol⁻¹ than **2a**.
8
9
10
11
12
13
14
15
16
17
18
19
20
21
22
23
24
25
26
27
28
29
30
31
32
33
34
35
36
37
38
39
40
41
42
43
44
45
46
47
48
49
50
51
52
53
54
55
56
57
58
59
60

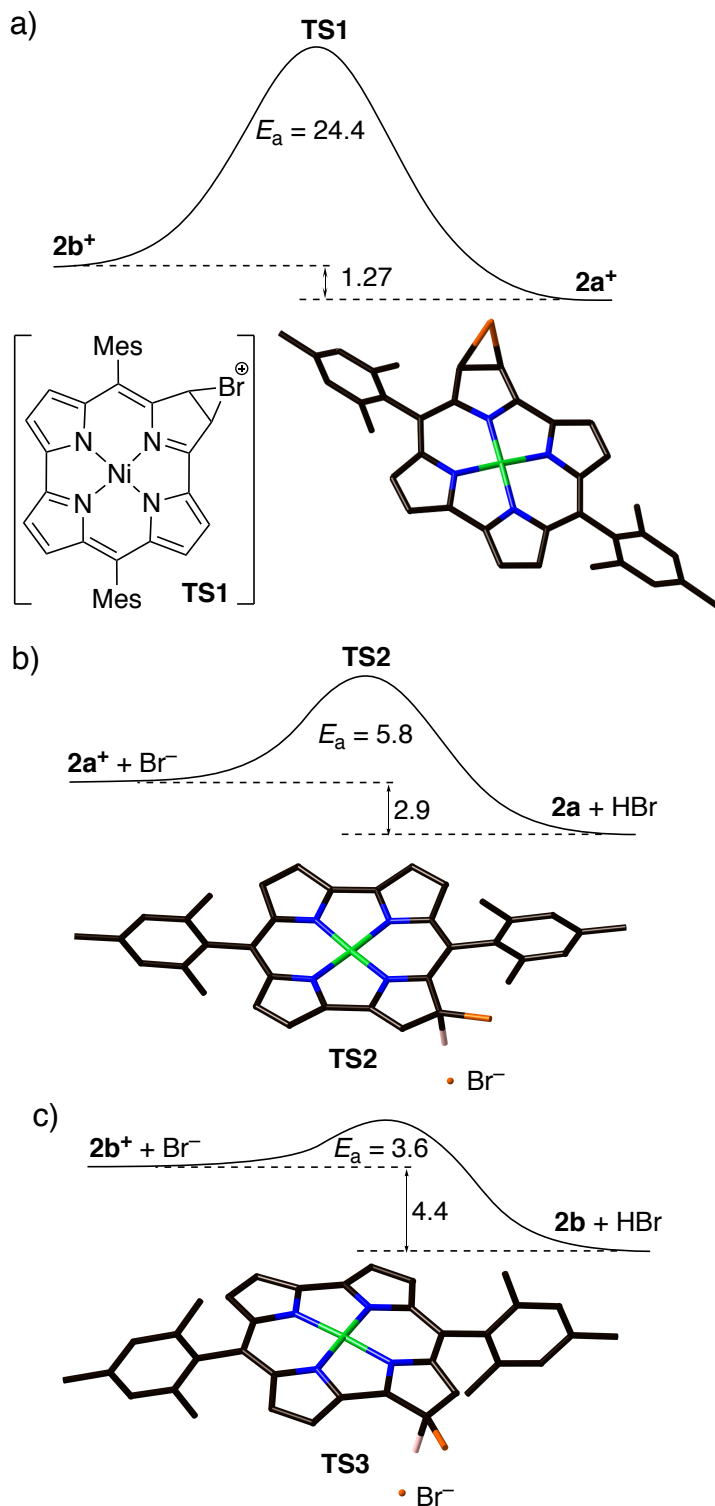


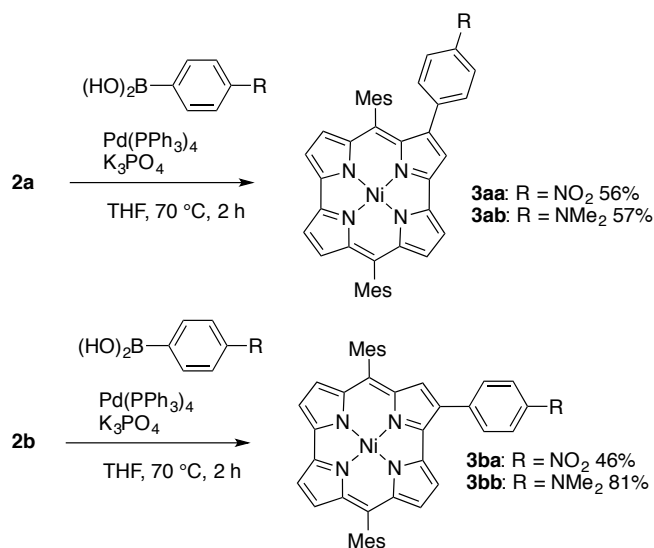
Figure 2. Calculated energy profiles and activation energies for a) migration between $2a^+$ and $2b^+$, b) deprotonation of $2a^+$, and c) deprotonation of $2b^+$. Calculations were performed at the

B3LYP/6-31+G(d,p)+SDD level. The solvent effect of THF was included by the PCM method. Energy values are shown in kcal mol⁻¹.

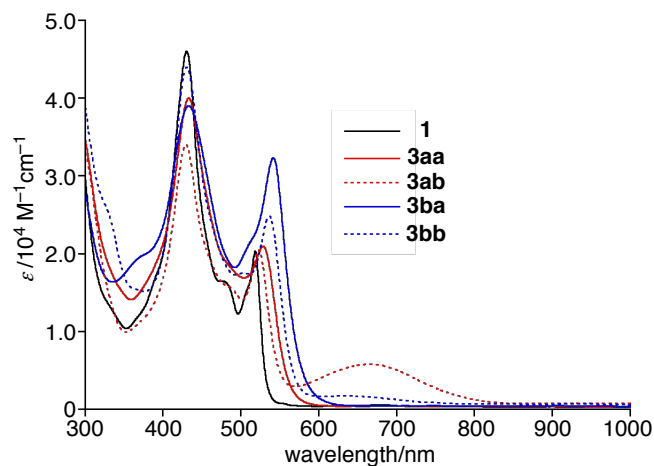
Suzuki–Miyaura Cross-coupling of bromonorcorroles and their properties

While several 3-functionalized norcorrole Ni(II) complexes have been reported, none of 2-functionalized norcorrole is precedent. With two different regioisomers of Ni(II) bromonorcorroles **2a** and **2b** in hand, we then introduced several functionalities on the periphery of norcorrole to investigate their substituent effect. Electron-rich and electron-deficient aryl groups were readily installed under the standard Suzuki–Miyaura coupling reaction conditions (Scheme 5). Arylated norcorroles were fully characterized by high-resolution mass and NMR spectra. In addition, the structure of **3ab** was clearly determined by the X-ray analysis (Figure S22). The introduced 3-dimethylaminophenyl group is tilted by 48.7° with respect to the adjacent pyrrole ring.

Scheme 5. Suzuki–Miyaura coupling of **2a** and **2b** with 4-nitrophenyl- and 4-dimethylaminophenylboronic acids.



1
2
3 The UV/vis absorption spectra of arylated products in dichloromethane are shown in Figure 3
4 along with that of the parent Ni(II) norcorrole **1**. The absorption spectra of **3aa** and **3ba** were
5 similar to that of **1** except small red-shifts of the absorption bands around 500 nm. In contrast, 3-
6 dimethylaminophenyl-substituted norcorroles **3ab** and **3bb** exhibited novel broad absorption
7 bands around 660 nm. The broad band in **3ab** was more evident than that in **3bb** but disappeared
8 upon the addition of trifluoroacetic acid to the solution (Figure S23). These results imply the
9 existence of intramolecular charge transfer interactions between the electron-donating
10 aminophenyl group and the norcorrole core. Time-dependent (TD)-DFT calculations of **3ab** and
11 **3bb** indicate that these absorption bands are originated from the HOMO-3 to LUMO transition
12 with significant charge transfer character (Figure S25). LUMO of **3bb** has a nodal position at the
13 2-position so that the intensity of this band was weaker than that in **3ab**.
14
15
16
17
18
19
20
21
22
23
24
25
26
27
28



29
30
31
32
33
34
35
36
37
38
39
40
41
42
43
44
45 **Figure 3.** UV/vis/NIR absorption spectra of **3aa**, **3ab**, **3ba**, and **3bb** in dichloromethane.

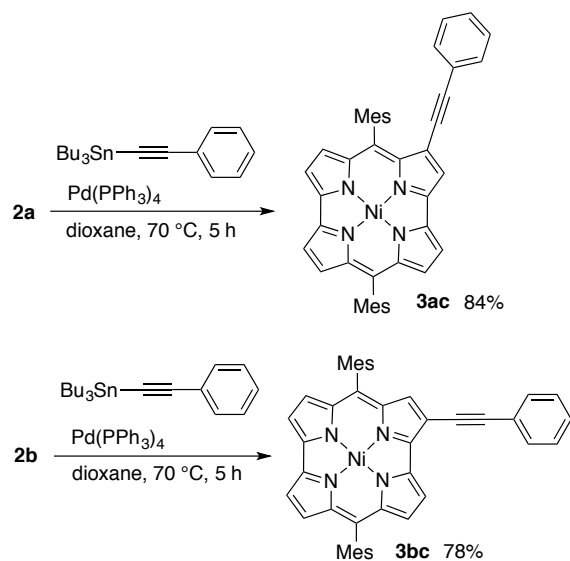
46
47
48 To obtain further insights on the substituent effect, the electrochemistry of arylated norcorroles
49 was examined with cyclic voltammetry (Figure S27). Oxidation and reduction potentials of **3aa**
50 and **3ba** were shifted anodically with respect to those of **1** due to the electron-withdrawing
51 nitrophenyl group. The electrochemical HOMO-LUMO gap was almost same as that of **1**. In
52
53
54
55
56
57
58
59
60

1
2
3 contrast, introduction of the dimethylaminophenyl group resulted in cathodic shifts in oxidation
4 and reduction potentials of **3ab** and the oxidation potential of **3bb**. However, the reduction
5 potential of **3bb** was unchanged from that of **1**, resulting in smaller HOMO–LUMO gap of **3bb**.
6
7
8 This is because the effect of the π -donating dimethylaminophenyl group on the LUMO level is
9 marginal because of the nodal position of LUMO at the 2-position of norcorrole.^{8e}
10
11
12
13
14
15
16
17

18 Alkynylation of Ni(II) norcorrole

19
20 Peripheral alkynyl moieties of porphyrinoids often enable efficient expansion of their π -
21 conjugation systems. Consequently, we attempted alkynylation of brominated norcorroles
22 through Sonogashira coupling. However, the reaction of **2a** with ethynylbenzene under standard
23 Sonogashira conditions (PdCl₂(PPh₃)₄, CuI, Et₃N/THF) afforded a complex mixture of many
24 products. We then found that Migita–Kosugi–Stille coupling with an alkynylstannane reagent
25 was quite effective to introduce a phenylethynyl groups to brominated norcorroles. The reaction
26 of **2a** and **2b** with tributyl(phenylethynyl)tin afford 2- and 3-phenylethynylnorcorroles **3ac** and
27
28
29
30
31
32
33
34
35
36
37 **3bc** in excellent yields (Scheme 6).

38
39 **Scheme 6.** Migita–Kosugi–Stille coupling of **2a** and **2b** with tributyl(phenylethynyl)stannane.
40
41
42
43
44
45
46
47
48
49
50
51
52
53
54
55
56
57
58
59
60



We also attempted exhaustive bromination of norcorrole **1**. Treatment of **1** with an excess amount of NBS (20 equiv) afforded octabromonorcorrole **4** along with octabromooxacorrole **5** (Scheme 7). Probably octabromooxacorrole was formed through oxidation of norcorrole **1** and brominated norcorroles with dioxygen in air.⁷ Because the low solubility of **4** hampered the purification with silica-gel column chromatography, we employed the mixture of these compounds for further functionalization without separation. Coupling of the mixture with an excess amount of tributyl(phenylethynyl)tin under the standard conditions provided octa(phenylethynyl)norcorrole **6** in 8% yield after purification. Although the alkynylated oxacorroles were detected in the reaction mixture by MS analysis, octa(phenylethynyl)oxacorrole could not be isolated because of difficult purification.

Scheme 7. Octabromination and octaalkynylation of **1**.

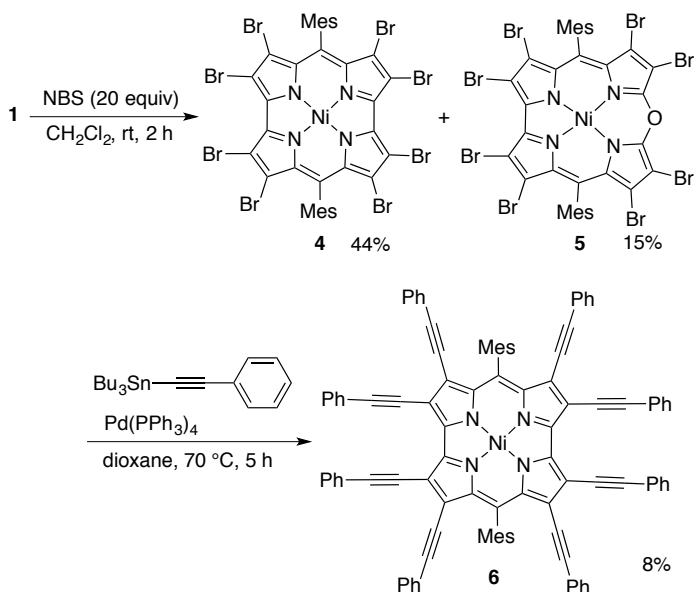


Figure 4 shows absorption spectra of series of alkynylated norcorroles **3ac**, **3bc**, and **6** along with that of **1** for comparison. While introduction of one phenylethynyl unit to **1** induced relatively small red shift (ca. 10 nm) in the absorption spectra, **6** exhibited substantially red-shifted and intensified absorption spectrum with broad absorption bands in the NIR region from 800 to 1600 nm. This NIR absorption band was characterized as HOMO-2→LUMO and HOMO-1→LUMO transitions on the basis of TD-DFT calculation (Figure S26). These molecular orbitals are substantially perturbed by the alkyne substituents. While degenerate HOMO-2 and HOMO-1 are delocalized over the norcorrole core and all of eight phenylethynyl units, LUMO is located on the norcorrole core and four ethynyl moieties at 3-, 7-, 12-, 16-positions (Figure S26b).

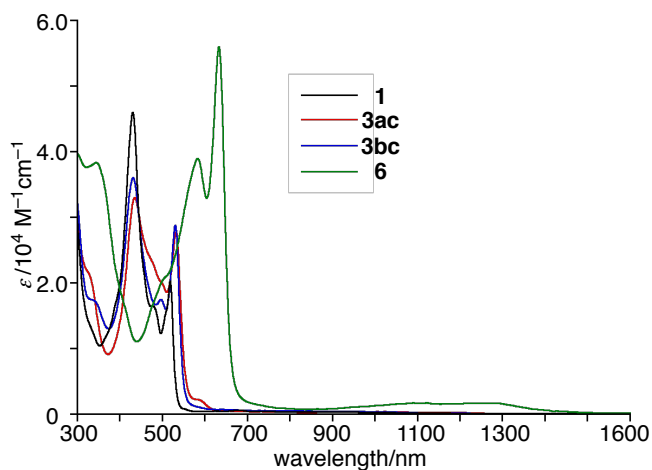


Figure 4. UV/vis/NIR absorption spectra of **1**, **3ac**, **3bc**, and **6** in dichloromethane.

The electrochemistry of alkynylated norcorroles **3ac**, **3bc**, and **6** was also investigated (Figure S28). Introduction of phenylethynyl groups induced anodic shifts due to the electron-withdrawing alkynyl substituents. In particular, octa(phenylethynyl)norcorrole **6** showed a rather high reduction potential, resulting in a small electrochemical HOMO–LUMO gap of 0.906 V. This result as well as the red-shifted broad NIR absorption band and the MO calculations indicate the effective expansion of π -conjugation over phenylethynyl substituents.

Conclusions

We have found hydrogen bromide-induced migration of the bromo substituent on norcorrole and developed a synthetic procedure for preparation of two regioisomeric Ni(II) bromonorcorroles. Treatment of Ni(II) dimesitylnorcorrole with NBS selectively afforded Ni(II) 3-bromonorcorrole, which was further converted into Ni(II) 2-bromonorcorrole upon treatment with hydrogen bromide. In addition, the reaction of Ni(II) norcorrole with an excess amount of NBS afforded the octabrominated product. The reaction mechanism of the bromination reaction of Ni(II) dimesitylnorcorrole was investigated by theoretical calculations. At low temperatures,

1
2
3 the electrophilic bromination reaction of norcorrole **1** selectively provides 3-bromonorcorrole **2a**
4 through more stable cationic intermediate **2a⁺**. Under highly acidic conditions at higher
5 temperatures, the whole processes are reversible, thus favoring the formation of
6 thermodynamically more stable product 2-bromonorcorrole **2b**. The brominated norcorroles
7 were employed for palladium-catalyzed cross-coupling reactions to provide a variety of
8 functionalized Ni(II) norcorroles. The optical and electrochemical properties of these substituted
9 Ni(II) norcorroles were investigated experimentally and theoretically. The present procedure for
10 selective bromination of Ni(II) norcorroles should be useful to prepare redox active and near IR
11 absorbing norcorrole derivatives.
12
13
14
15
16
17
18
19
20
21
22
23
24
25
26

27 Experimental Section

28
29 **Instrumentation and Materials:** ¹H NMR (500 MHz) and ¹³C NMR (126 MHz) spectra were
30 recorded on a Bruker AVANCE III HD spectrometer, and chemical shifts were reported as the
31 delta scale in ppm relative to CHCl₃ ($\delta = 7.260$ ppm) for ¹H NMR and CDCl₃ ($\delta = 77.16$ ppm)
32 for ¹³C NMR. UV/vis/NIR absorption spectra were recorded on a Shimadzu UV-2550 or JASCO
33 V670 spectrometer. High-resolution mass spectra were recorded on a Bruker microTOF using
34 positive mode ESI-TOF method for acetonitrile solutions. X-ray diffraction data were taken on
35 a Bruker D8 QUEST X-ray diffractometer with ImS microfocus X-ray source and a large area
36 (10 cm × 10 cm) CMOS detector (PHOTON 100). Unless otherwise noted, materials obtained
37 from commercial suppliers were used without further purification.
38
39
40
41
42
43
44
45
46
47
48
49
50

51 **Synthesis of 2a:** A solution of Ni(II) dimesitylnorcorrole **1** (116 mg, 201 μ mol) in THF (80
52 mL) was cooled to -60 °C. A solution of *N*-bromosuccinimide (37.8 mg, 212 μ mol) in THF (20
53 mL) was added dropwise and the mixture was stirred at -60 °C for 1.5 h. Acetone (10 mL) was
54
55
56
57
58
59
60

1
2
3 then added and the mixture was warmed to room temperature. An aqueous NaHCO₃ solution was
4 added and the mixture was extracted with ethyl acetate (20 mL × 3). The combined organic
5 layers were washed with water and brine, and dried over Na₂SO₄. After removing the solvent, the
6 residue was purified by silica-gel column chromatography (hexane/CH₂Cl₂ = 4/1 as an eluent).
7
8 The product was further purified by recrystallization (CH₂Cl₂/MeOH) to afford Ni(II) 3-bromo-
9
10 5,14-dimesitylnorcorrole **2a** (94.1 mg, 143 μmol) as black crystals in 72% yield. Mp > 300 °C.
11
12
13
14
15
16
17
18
19
20
21
22
23
24
25
26
27
28
29
30
31
32
33
34
35
36
37
38
39
40
41
42
43
44
45
46
47
48
49
50
51
52
53
54
55
56
57
58
59
60

¹H NMR (500 MHz, CDCl₃): δ = 6.27 (s, 2H, Mes), 6.27 (s, 2H, Mes), 2.87 (s, 6H, *ortho*-Mes), 2.86 (s, 6H, *ortho*-Mes), 1.87 (d, *J* = 4.5 Hz, 1H, β-CH), 1.84 (s, 3H, *para*-Mes), 1.83 (s, 3H, *para*-Mes), 1.76 (d, *J* = 4.5 Hz, 1H, β-CH), 1.73 (d, *J* = 4.5 Hz, 1H, β-CH), 1.69 (d, *J* = 4.0 Hz, 1H, β-CH), 1.69 (s, 1H, β-CH), 1.66 (d, *J* = 4.0 Hz, 1H, β-CH), 1.60 (d, *J* = 4.5 Hz, 1H, β-CH) ppm. ¹³C NMR (500 MHz, CDCl₃): δ = 170.2, 169.7, 166.8, 165.5, 159.4, 158.4, 148.6, 148.1, 148.0, 142.8, 137.2, 137.1, 133.8, 133.5, 131.6, 131.0, 128.9, 128.2, 128.0, 125.8, 124.9, 116.8, 116.0, 115.2, 114.9, 20.8, 20.7, 17.8, 17.8 ppm. UV/vis (CH₂Cl₂) λ_{max} (ε [M⁻¹ cm⁻¹]): 431 (45000), 480 (18000), 518 (20000) nm. HRMS (ESI-TOF) m/z: [M]⁺ Calcd for C₃₆H₂₉BrN₄Ni 656.0903; Found 656.0873.

Synthesis of 2b: To a solution of **2a** (98.4 mg, 150 μmol) in dry THF (15 mL) was added a solution of HBr in acetic acid (190 mg) under N₂ atmosphere. The mixture was stirred at room temperature for 30 min. A NaHCO₃ solution was added to quench the reaction and the mixture was extracted with ethyl acetate (20 mL × 3). The combined organic layers were washed with water and brine, and dried over Na₂SO₄. After removing the solvent, the residue was purified by silica-gel column chromatography (hexane/CH₂Cl₂ = 9/1 as an eluent). The product was further purified by recrystallization (CHCl₃/MeOH) to afford Ni(II) 2-bromo-5,14-dimesitylnorcorrole **2b** (51.3 mg, 78.1 μmol) as black crystals in 52% yield. Mp > 300 °C. ¹H NMR (500 MHz,

1
2
3
4
5
6
7
8
9
10
11
12
13
14
15
16
17
18
19
20
21
22
23
24
25
26
27
28
29
30
31
32
33
34
35
36
37
38
39
40
41
42
43
44
45
46
47
48
49
50
51
52
53
54
55
56
57
58
59
60

CDCl₃): δ = 6.27 (s, 4H, Mes), 2.89 (s, 6H, *ortho*-Mes), 2.88 (s, 6H, *ortho*-Mes), 1.83 (s, 3H, *para*-Mes), 1.83 (s, 3H, *para*-Mes), 1.82 (d, J = 4.5 Hz, 1H, β -CH), 1.78 (d, J = 4.5 Hz, 1H, β -CH), 1.72 (d, J = 4.5 Hz, 1H, β -CH), 1.64 (d, J = 4.0 Hz, 1H, β -CH), 1.59 (d, J = 4.0 Hz, 1H, β -CH), 1.56 (d, J = 4.0 Hz, 1H, β -CH), 1.56 (s, 1H, β -CH) ppm. ¹³C NMR (500 MHz, CDCl₃): δ = 172.5, 169.2, 165.3, 162.7, 159.0, 158.2, 148.3, 148.2, 147.2, 137.3, 137.1, 133.4, 132.6, 131.7, 128.3, 128.3, 128.2, 126.7, 125.8, 125.4, 116.5, 116.2, 114.9, 100.1, 20.7, 17.7, 17.7 ppm. UV/vis (CH₂Cl₂) λ_{\max} (ϵ [M⁻¹ cm⁻¹]): 432 (42000), 480 (18000), 519 (20000) nm. HRMS (ESI-TOF) m/z : [M]⁺ Calcd for C₃₆H₂₉BrN₄Ni 656.0903; Found 656.0928.

Synthesis of 3aa: A Schlenk flask containing **2a** (13.8 mg, 21.0 μ mol), 4-nitrophenylboronic acid (43.9 mg, 263 μ mol), Pd(PPh₃)₄ (4.81 mg, 4.16 μ mol), and K₃PO₄ (109 mg, 513 μ mol) was filled with N₂ and dry THF (2.0 mL) was added. The solution was stirred at 70 °C for 2 h. After cooling down, the resulting mixture was passed through a short pad of silica-gel with CHCl₃ and the solution concentrated in vacuo. The residue was purified by silica-gel column chromatography (hexane/CH₂Cl₂ = 7/3 as eluent). The product was further purified by recrystallization (CHCl₃/MeOH) to afford Ni(II) 3-(4-nitrophenyl)-5,14-dimesitylnorcorrole **3aa** (8.19 mg, 11.7 μ mol, 56%) as dark brown crystals. Mp > 300 °C. ¹H NMR (500 MHz, CDCl₃): δ = 7.10 (*pseudo*-d, J = 8.5 Hz, 2H, Ph), 6.28 (s, 2H, Mes), 5.88 (s, 2H, Mes), 5.54 (*pseudo*-d, 2H, J = 8.5 Hz, Ph), 2.90 (s, 6H, *ortho*-Mes), 2.74 (s, 6H, *ortho*-Mes), 1.84 (d, J = 4.5 Hz, 1H, β -CH), 1.84 (d, J = 4.0 Hz, 1H, β -CH), 1.84 (s, 3H, *para*-Mes), 1.77 (d, J = 4.0 Hz, 1H, β -CH), 1.71 (d, J = 4.5 Hz, 1H, β -CH), 1.66 (d, J = 4.0 Hz, 1H, β -CH), 1.63 (d, J = 4.5 Hz, 2H, β -CH), 1.61 (s, 3H, *para*-Mes), 1.60 (s, 1H, β -CH) ppm. ¹³C NMR (500 MHz, CDCl₃): δ = 170.7, 170.0, 166.0, 164.9, 159.1, 157.6, 148.4, 148.0, 148.0, 145.2, 144.3, 143.8, 138.9, 138.0, 137.1, 133.6, 133.5, 132.4, 131.4, 128.7, 128.2, 127.9, 125.8, 125.8, 125.1, 121.3, 116.2, 115.4, 114.9, 114.8, 20.7,

20.3, 17.9, 17.8 ppm. UV/vis (CH₂Cl₂) λ_{max} (ε [M⁻¹ cm⁻¹]): 433(40000), 529(21000) nm. HRMS (ESI-TOF) m/z: [M]⁺ Calcd for C₄₂H₃₃N₅NiO₂ 697.1982; Found 697.1980.

Synthesis of 3ab: A Schlenk flask containing **2a** (13.1 mg, 20.0 μmol), 4-*N,N*-dimethylaminophenylboronic acid (40.0 mg, 243 μmol), Pd(PPh₃)₄ (5.21 mg, 4.50 μmol), and K₃PO₄ (107 mg, 502 μmol) was filled with N₂ and dry THF (2.0 mL) was added. The solution was stirred at 70 °C for 2 h. After cooling down, the resulting mixture was passed through a short pad of silica-gel with CHCl₃ and the solution concentrated in vacuo. The residue was purified by silica-gel column chromatography (hexane/CH₂Cl₂ = 7/3 as eluent). The product was purified by recrystallization (CHCl₃/MeOH) to afford Ni(II) 3-(4-*N,N*-dimethylaminophenyl)-5,14-dimesitylnorcorrole **3ab** (7.84 mg, 11.3 μmol, 57%) as black crystals. Mp > 300 °C. ¹H NMR (500 MHz, CDCl₃): δ = 6.29 (s, 2H, Mes), 5.93 (s, 2H, Mes), 5.57 (*pseudo*-d, *J* = 9.0 Hz, 2H, Ph), 5.29 (*pseudo*-d, *J* = 9.0 Hz, 2H, Ph), 2.89 (s, 6H, *ortho*-Me), 2.72 (s, 6H, *ortho*-Me), 2.53 (s, 6H, Me), 1.88 (d, *J* = 4.5 Hz, 1H, β-CH), 1.84 (s, 3H, *para*-Me), 1.73 (d, *J* = 4.0 Hz, 1H, β-CH), 1.71 (d, *J* = 4.0 Hz, 1H, β-CH), 1.68 (d, *J* = 4.0 Hz, 1H, β-CH), 1.67 (s, 1H, β-CH), 1.66 (d, *J* = 4.0 Hz, 1H, β-CH), 1.59 (d, *J* = 4.0 Hz, 1H, β-CH) ppm. ¹³C NMR (500 MHz, CDCl₃): δ = 170.1, 170.4, 164.0, 162.4, 157.7, 156.9, 153.6, 149.4, 148.4, 147.7, 147.2, 144.8, 136.9, 136.3, 133.7, 133.7, 131.7, 128.1, 127.7, 127.1, 127.0, 126.6, 126.2, 125.1, 120.0, 115.6, 115.5, 114.0, 113.7, 109.7, 40.3, 20.7, 20.5, 17.9, 17.8 ppm. UV/vis (CH₂Cl₂) λ_{max} (ε [M⁻¹ cm⁻¹]): 430 (34000), 523 (20000), 665 (5800) nm. HRMS (ESI-TOF) m/z: [M]⁺ Calcd for C₄₄H₃₉N₅Ni 695.2554; Found 695.2528.

Synthesis of 3ba: A Schlenk flask containing 2-bromo-5,14-dimesitylnorcorrole **2b** (13.4 mg, 20.5 μmol), 4-nitrophenylboronic acid (41.7 mg, 250 μmol), Pd(PPh₃)₄ (5.66 mg, 4.90 μmol), and K₃PO₄ (108 mg, 508 μmol) was filled with N₂ and dry THF (2.0 mL) was added. The

1
2
3 solution was stirred at 70 °C for 2 h. After cooling down, the resulting mixture was passed
4 through a short pad of silica-gel with CHCl₃ and the solution was concentrated in vacuo. The
5 residue was purified by silica-gel column chromatography (hexane/CH₂Cl₂ = 7/3 as eluent). The
6 product was further purified by recrystallization (CHCl₃/MeOH) to afford Ni(II) 2-(4-
7 nitrophenyl)-5,14-dimesitylnorcorrole **3ba** (6.67 mg, 9.55 μmol, 46%) as dark brown crystals.
8
9
10
11
12
13
14
15
16
17
18
19
20
21
22
23
24
25
26
27
28
29
30
31
32
33
34
35
36
37
38
39
40
41
42
43
44
45
46
47
48
49
50
51
52
53
54
55
56
57
58
59
60
Mp > 300 °C. ¹H NMR (500 MHz, CDCl₃): δ = 7.42 (*pseudo*-d, *J* = 9.0 Hz, 2H, Ph), 6.35 (s, 2H, Mes), 6.31 (s, 2H, Mes), 5.36 (*pseudo*-d, 2H, *J* = 9.0 Hz, Ph), 2.88 (s, 6H, *ortho*-Mes), 2.86 (s, 6H, *ortho*-Mes), 2.09 (d, *J* = 4.5 Hz, 1H, β-CH), 1.98 (s, 1H, β-CH), 1.97 (d, *J* = 4.0 Hz, 1H, β-CH), 1.94 (d, *J* = 4.5 Hz, 1H, β-CH), 1.93 (d, *J* = 4.5 Hz, 1H, β-CH), 1.88 (s, 3H, *para*-Mes), 1.87 (d, *J* = 4.0 Hz, 1H, β-CH), 1.86 (s, 3H, *para*-Mes), 1.83 (d, *J* = 4.5 Hz, 1H, β-CH) ppm. ¹³C NMR (500 MHz, CDCl₃): δ = 171.6, 169.0, 166.0, 162.9, 159.5, 158.9, 148.3, 148.1, 147.9, 147.7, 145.1, 137.8, 137.4, 137.3, 133.6, 133.5, 132.3, 131.5, 129.3, 129.1, 128.4, 128.3, 125.9, 125.8, 124.3, 123.3, 121.7, 116.9, 116.4, 115.3, 20.7, 20.7, 17.9, 17.8 ppm. UV/vis (CH₂Cl₂) λ_{max} (ε [M⁻¹ cm⁻¹]): 433 (39000), 542 (32000) nm. HRMS (ESI-TOF) *m/z*: [M]⁺ Calcd for C₄₂H₃₃N₅NiO₂ 697.1982; Found 697.1958.

Synthesis of 3bb: A Schlenk flask containing **2b** (13.4 mg, 20.5 μmol), 4-*N,N*-dimethylaminophenylboronic acid (40.3 mg, 244 μmol), Pd(PPh₃)₄ (5.63 mg, 4.87 μmol), and K₃PO₄ (108 mg, 508 μmol) was filled with N₂ and dry THF (2.0 mL) was added. The solution was stirred at 70 °C for 2 h. After cooling down, the resulting mixture was passed through a short pad of silica-gel with CHCl₃ and the solution was concentrated in vacuo. The residue was purified by silica-gel column chromatography (hexane/CH₂Cl₂ = 7/3 as eluent). The product was further purified by recrystallization (CHCl₃/MeOH) to afford Ni(II) 3-(4-*N,N*-dimethylaminophenyl)-5,14-dimesitylnorcorrole **3bb** (7.84 mg, 11.3 μmol, 81%) as black crystals.

1
2
3 Mp > 300 °C. ¹H NMR (500 MHz, CDCl₃): δ = 6.25 (s, 2H, Mes), 6.24 (s, 2H, Mes), 5.57
4 (pseudo-d, J = 9.0 Hz, 2H, Ph), 5.29 (pseudo-d, J = 9.0 Hz, 2H, Ph), 2.89 (s, 6H, *ortho*-Me), 2.72
5 (s, 6H, *ortho*-Me), 2.53 (s, 6H, Me), 1.88 (d, J = 4.5 Hz, 1H, β-CH), 1.84 (s, 3H, *para*-Me), 1.73
6 (d, J = 4.0 Hz, 1H, β-CH), 1.71 (d, J = 4.0 Hz, 1H, β-CH), 1.68 (d, J = 4.0 Hz, 1H, β-CH), 1.67
7 (s, 1H, β-CH), 1.66 (d, J = 4.0 Hz, 1H, β-CH), 1.59 (d, J = 4.0 Hz, 1H, β-CH) ppm. ¹³C NMR
8 (500 MHz, CDCl₃): δ = 170.1, 170.4, 164.0, 162.4, 157.7, 156.9, 153.6, 149.4, 148.4, 147.7,
9 147.2, 144.8, 136.9, 136.3, 133.7, 133.7, 131.7, 128.1, 127.7, 127.1, 127.0, 126.6, 126.2, 125.1,
10 120.0, 115.6, 115.5, 114.0, 113.7, 109.7, 40.3, 20.7, 20.5, 17.9, 17.8 ppm. UV/vis (CH₂Cl₂) λ_{max}
11 (ε [M⁻¹ cm⁻¹]): 431 (44000), 537 (25000) nm. HRMS (ESI-TOF) m/z: [M]⁺ Calcd for C₄₄H₃₉N₅Ni
12 695.2554; Found 695.2548.

13
14
15
16
17
18
19
20
21
22
23
24
25
26
27 **Synthesis of 3ac:** A Schlenk flask containing **2a** (13.2 mg, 20.1 μmol) and Pd(PPh₃)₄ (5.0 mg,
28 4.3 μmol) was filled with N₂ and dry dioxane (4.0 mL) was added and stirred at room
29 temperature for 15 min. Tributyl(phenylethynyl)tin was added dropwise (25 μL) and the mixture
30 was stirred at 70 °C for 5 h. After cooling down, the resulting mixture was passed through a
31 short pad of silica-gel with CH₂Cl₂ and the solution concentrated in vacuo. The residue was
32 purified by silica-gel column chromatography (10% w/w anhydrous K₂CO₃/silica-gel;
33 hexane/CH₂Cl₂ = 7/3 as eluent) to afford Ni(II) 3-(phenylethynyl)-5,14-dimesitylnorcorrole **3ac**
34 (11.4 mg, 16.9 μmol, 84%) as black crystals. Mp > 300 °C. ¹H NMR (500 MHz, CDCl₃): δ =
35 6.97–6.93 (m, 1H, Ph), 6.89–6.86 (m, 2H, Ph), 6.29 (s, 2H, Mes), 6.29–6.27 (m, 2H, Ph), 6.25 (s,
36 2H, Mes), 2.91 (s, 6H, *ortho*-Me), 2.86 (s, 6H, *ortho*-Me), 2.53 (s, 6H, Me), 1.92 (d, J = 4.5 Hz,
37 1H, β-CH), 1.85 (d, J = 4.5 Hz, 1H, β-CH), 1.85 (s, 3H, *para*-Me), 1.83 (s, 1H, β-CH), 1.80 (d, J
38 = 4.5 Hz, 1H, β-CH), 1.76 (s, 3H, *para*-Me), 1.76 (d, J = 4.0 Hz, 1H, β-CH), 1.72 (d, J = 4.0 Hz,
39 1H, β-CH), 1.71 (d, J = 4.5 Hz, 1H, β-CH) ppm. ¹³C NMR (500 MHz, CDCl₃): δ = 170.4, 169.8,
40 41 42 43 44 45 46 47 48 49 50 51 52 53 54 55 56 57 58 59 60

1
2
3 166.1, 165.0, 159.0, 157.7, 148.6, 147.9, 147.8, 147.3, 137.1, 137.0, 134.2, 133.6, 131.7, 131.3,
4
5 131.0, 128.5, 128.2, 128.0, 27.6, 127.4, 26.0, 125.6, 123.4, 122.8, 118.0, 116.0, 15.3, 114.9, 95.1,
6
7 80.9, 21.0, 20.6, 27.8, 17.8 ppm. UV/vis (CH₂Cl₂) λ_{max} (ε [M⁻¹ cm⁻¹]): 435(33000), 533(28000),
8
9 578(2300) nm. HRMS (ESI-TOF) m/z: [M]⁺ Calcd for C₄₄H₃₄N₄Ni 676.2137; Found 676.2137.

10
11
12 **Synthesis of 3bc:** A Schlenk flask containing **2b** (13.4 mg, 20.4 μmol) and Pd(PPh₃)₄ (4.8 mg,
13
14 4.2 μmol) was filled with N₂ and dry dioxane (4.0 mL) was added and stirred at room
15
16 temperature for 15 min. Tributyl(phenylethynyl)tin was added dropwise (25 μL) and the mixture
17
18 was stirred at 70 °C for 5 h. After cooling down, the resulting mixture was passed through a
19
20 short pad of silica-gel with CH₂Cl₂ and the solution concentrated in vacuo. The residue was
21
22 purified by silica-gel column chromatography (10% w/w anhydrous K₂CO₃/silica-gel;
23
24 hexane/CH₂Cl₂ = 7/3 as eluent) to afford Ni(II) 2-(phenylethynyl)-5,14-dimesitylnorcorrole **3bc**
25
26 (10.8 mg, 16.0 μmol, 78%) as black crystals. Mp > 300 °C. ¹H NMR (500 MHz, CDCl₃): δ =
27
28 7.01–6.98 (m, 1H, Ph), 6.96–6.92 (m, 2H, Ph), 6.64–6.62 (m, 2H, Ph), 6.30 (s, 2H, Mes), 6.29 (s,
29
30 2H, Mes), 2.89 (s, 6H, *ortho*-Me), 2.89 (s, 6H, *ortho*-Me), 1.94 (d, *J* = 4.5 Hz, 1H, β-CH), 1.89
31
32 (d, *J* = 4.5 Hz, 1H, β-CH), 1.86 (d, *J* = 4.5 Hz, 1H, β-CH), 1.85 (s, 6H, Me), 1.85 (s, 3H, *para*-
33
34 Me), 1.82 (s, 1H, β-CH), 1.77 (d, *J* = 4.5 Hz, 1H, β-CH), 1.72 (d, *J* = 4.0 Hz, 1H, β-CH), 1.69 (d,
35
36 *J* = 4.0 Hz, 1H, β-CH) ppm. ¹³C NMR (500 MHz, CDCl₃): δ = 171.5, 169.3, 166.2, 165.4, 158.9,
37
38 158.4, 148.5, 148.0, 147.8, 146.8, 137.2, 137.1, 133.6, 132.2, 131.6, 130.7, 129.3, 128.6, 128.3,
39
40 128.2, 128.0, 127.5, 126.0, 125.7, 123.0, 116.5, 116.3, 114.9, 109.6, 90.1, 79.8, 20.7, 17.8, 17.8
41
42 ppm. UV/vis (CH₂Cl₂) λ_{max} (ε [M⁻¹ cm⁻¹]): 432 (36000), 498 (20000), 531 (32000), 646 (5100)
43
44 nm. HRMS (ESI-TOF) m/z: [M]⁺ Calcd for C₄₄H₃₄N₄Ni 676.2137; Found 676.2138.

45
46
47
48
49
50
51
52
53 **Synthesis of 4:** To a solution of **1** (35.2 mg, 60.9 μmol) in dry CH₂Cl₂ (15 mL) was added a
54
55 solution of *N*-bromosuccinimide (214 mg, 1.20 mmol) in CH₂Cl₂ (30 mL) under argon
56
57
58
59
60

1
2
3 atmosphere in a glovebox. The mixture was stirred at room temperature for 2 h. After removing
4
5 the solvent, the residue was purified by silica-gel column chromatography (CHCl₃ as eluent).
6
7
8 The product was further purified by recrystallization (CHCl₃/MeOH). Ni(II) octabromo-5,14-
9
10 dimesitylnorcorrole **4** and Ni(II) octabromo-5,15-dimesityl-10-oxacorrole **5** were obtained as an
11
12 inseparable mixture as a black solid. The yield of **4** was determined on the basis of the NMR
13
14 analysis. Mp > 300 °C. ¹H NMR (500 MHz, CDCl₃): δ = 6.31 (s, 4H, Mes), 2.81 (s, 12H, *ortho*-
15
16 Me), 1.89 (s, 6H, *para*-Me) ppm. The ¹³C NMR spectrum of **4** was difficult to be measured due
17
18 to the low solubility. HRMS (ESI-TOF) m/z: [M]⁺ Calcd for C₃₆H₂₂Br₈N₄Ni 1207.4587; Found
19
20 1207.4585.
21
22
23

24
25 **Synthesis of 6:** A Schlenk flask containing a mixture of octabromonorcorrole **4** and
26
27 octabromooxacorrole **5** (25.3 mg, **4:5** = 3:1) and Pd(PPh₃)₄ (9.76 mg, 8.44 μmol) was filled with
28
29 N₂ and dry dioxane (15 mL) was added and stirred at room temperature for 15 min.
30
31 Tributyl(phenylethynyl)tin was added dropwise (170 μL) and the mixture was stirred at 70 °C
32
33 for 5 h. After cooling down, the resulting mixture was passed through a short pad of silica-gel
34
35 with CH₂Cl₂ and the solution concentrated in vacuo. The residue was purified by silica-gel
36
37 column chromatography (10% w/w anhydrous K₂CO₃/silica-gel; hexane/CH₂Cl₂ = 3/2 as eluent)
38
39 to afford Ni(II) octa(phenylethynyl)-5,14-dimesitylnorcorrole **6** (1.81 mg, 1.31 μmol, 8%) as
40
41 dark purple crystals. Mp > 300 °C. ¹H NMR (500 MHz, CDCl₃): δ = 7.05–7.02 (m, 4H, Ph),
42
43 6.97–6.90 (m, 12H, Ph), 6.75–6.72 (m, 8H, Ph), 6.68–6.66 (m, 8H Ph), 6.49–6.48 (m, 4H, Ph),
44
45 6.40 (s, 4H, Mes), 2.91 (s, 12H, *ortho*-Me), 1.86 (s, 6H, *para*-Me) ppm. ¹³C NMR (500 MHz,
46
47 CDCl₃): δ = 166.1, 157.1, 146.2, 138.0, 135.2, 131.5, 131.2, 129.4, 128.2, 127.8, 127.7, 125.1,
48
49 122.7, 122.6, 116.3, 102.4, 96.2, 80.8, 79.1, 20.8, 18.2 ppm. UV/vis (CH₂Cl₂) λ_{max} (ε [M⁻¹ cm⁻¹]):
50
51
52
53
54
55
56
57
58
59
60

345 (38000), 583 (39000), 633 (56000), 1104 (1700), 1234 (1700) nm. HRMS (ESI-TOF) m/z :
[M]⁺ Calcd for C₁₀₀H₆₂N₄Ni 1377.4355; Found 1377.4342.

X-ray diffraction analysis: X-ray data for **2a** and **2b** were obtained using a Rigaku CCD diffractometer (Saturn 724 with MicroMax-007) with Varimax Mo optics using graphite monochromated Mo-K α radiation ($\lambda = 0.71075 \text{ \AA}$). X-ray data for **3ab** were obtained using a Bruker D8 QUEST X-ray diffractometer with an I μ S microfocus X-ray source and a large area CMOS detector (PHOTON 100). Crystallographic data for **2a**, **2b**, and **3ab** have been deposited with the Cambridge Crystallographic Data Centre.

Crystallographic data for 2a (CCDC-1516103): Single crystals were obtained by vapor diffusion of methanol into a chloroform solution. C₃₆H₂₉BrN₄Ni, $M_w = 656.25$, monoclinic, $P2_1/c$, $a = 13.1619(8) \text{ \AA}$, $b = 13.8635(4) \text{ \AA}$, $c = 8.2762(3) \text{ \AA}$, $\beta = 101.230(5)^\circ$, $V = 1481.24(12) \text{ \AA}^3$, $Z = 2$, $R_1 = 0.0608$ ($I > 2.0 \sigma(I)$), $R_w = 0.1702$ (all data), GOF = 1.087.

Crystallographic data for 2b (CCDC-1516102): Single crystals were obtained by vapor diffusion of methanol into a chloroform solution. C₃₆H₂₉BrN₄Ni, $M_w = 656.25$, monoclinic, $P2_1/c$, $a = 12.6966(3) \text{ \AA}$, $b = 27.8406(7) \text{ \AA}$, $c = 8.1912(2) \text{ \AA}$, $\beta = 98.977(2)^\circ$, $V = 2859.97(12) \text{ \AA}^3$, $Z = 4$, $R_1 = 0.0445$ ($I > 2.0 \sigma(I)$), $R_w = 0.1403$ (all data), GOF = 1.272.

Crystallographic data for 3ab (CCDC-1516104): Single crystals were obtained by vapor diffusion of methanol into a dichloromethane solution. C₄₅H₄₁Cl₂N₅Ni, $M_w = 781.44$, monoclinic, $P2_1/c$, $a = 9.7230(4) \text{ \AA}$, $b = 25.486(11) \text{ \AA}$, $c = 15.9516(5) \text{ \AA}$, $\beta = 106.565(4)^\circ$, $V = 3788.8(3) \text{ \AA}^3$, $Z = 4$, $R_1 = 0.0596$ ($I > 2.0 \sigma(I)$), $R_w = 0.1504$ (all data), GOF = 1.065.

Cyclic Voltammetry: Cyclic voltammograms of compounds were recorded on ALS electrochemical analyzer 612C. Measurements were performed in freshly distilled dichloromethane with tetrabutylammonium hexafluorophosphate as electrolyte. A three-

1
2
3 electrode system was used and consisted of a grassy carbon working electrode, a platinum wire
4 and Ag/AgClO₄ as the reference electrode. All potentials are referenced to the potential of
5
6
7
8 ferrocene/ferrocenium cation couple.
9

10 **Theoretical calculations:** All calculations were carried out using the *Gaussian 09* program.¹⁴
11
12 Full optimizations were performed with Becke's three-parameter hybrid exchange functional and
13
14 the Lee–Yang–Parr correlation functional (B3LYP) and a basis set consisting of SDD for Ni and
15
16 6-31G(d) for the rest. Geometries of **2a** and **2b** were obtained from their X-ray crystal structures.
17
18 For the calculation of the reaction pathway, rough transition state geometries were obtained
19
20 using the *Reaction plus Pro* software package,¹⁵ based on the nudged elastic band method.¹⁶ The
21
22 ground and transition state geometries were fully optimized at the B3LYP/6-31+G(d,p)+SDD
23
24 level without any symmetry restriction. The solvent effect of THF was included on the basis of
25
26 the PCM method using the `scrf = iefpcm` keyword. Zero-point energy and thermal energy
27
28 corrections were conducted for all optimized structures, and the sums of electronic and thermal
29
30 free energies were obtained. The zero-point energies were not scaled, and the enthalpic
31
32 corrections were made at 298.150 K. The transition states gave single imaginary frequency. The
33
34 calculated absorption wavelengths and oscillator strengths were obtained with the TD-DFT
35
36 method at the B3LYP/6-31G(d)+SDD level for the optimized structures at the same level of
37
38 theory.
39
40
41
42
43
44
45
46
47

48 ASSOCIATED CONTENT

49 Supporting Information.

50
51
52 The Supporting Information is available free of charge on the ACS Publications website at DOI:
53
54
55
56
57
58
59
60
XXXXX.

1
2
3
4
5
6
7
8
9
10
11
12
13
14
15
16
17
18
19
20
21
22
23
24
25
26
27
28
29
30
31
32
33
34
35
36
37
38
39
40
41
42
43
44
45
46
47
48
49
50
51
52
53
54
55
56
57
58
59
60

Crystallographic data for **2a** (CIF)

Crystallographic data for **2b** (CIF)

Crystallographic data for **3ab** (CIF)

NMR spectra, UV/vis absorption spectra, cyclic voltammograms, and results of DFT calculations (PDF)

AUTHOR INFORMATION

Corresponding Author

*E-mail: hshino@chembio.nagoya-u.ac.jp

Notes

The authors declare no competing financial interest.

ACKNOWLEDGMENT

This work was supported by JSPS KAKENHI Grant Numbers JP26102003 and JP17H01190.

H.S. gratefully acknowledges the Murata Science Foundation for financial support.

REFERENCES

(1) (a) Schnurch, M.; Spina, M.; Khan, A. F.; Mihovilovic, M. D.; Stanetty, P. *Chem. Soc. Rev.* **2007**, *36*, 1046. (b) Schlosser, M. *Angew. Chem. Int. Ed.* **2005**, *44*, 376. (c) Duan, X. F.; Zhang, Z. B. *Heterocycles* **2005**, *65*, 2005.

(2) (a) Reverdin, F. *Ber.* **1896**, *29*, 997. (b) Robinson, G. M. *J. Chem. Soc., Transactions* **1916**, *109*, 1078. (c) Butler, A. R.; Sanderson, A. P. *J. Chem. Soc. Perkin Trans. 2* **1972**, 989. (d) Brittain, J. M.; de la Mare, P. B. D.; Newman, P. A. *Tetrahedron Lett.* **1980**, *21*, 4111. (e) Jacquesy, J.-C.; Jouannetaud, M.-P. *Tetrahedron Lett.* **1982**, *23*, 1673. (f) Giles, R. G. F.; Green,

1
2
3 I. R.; Knight, L. S.; Son, V. R. L.; Mitchell, P. R. K.; Yorke, S. C. *J. Chem. Soc. Perkin Trans. 1*
4
5 **1994**, 853.

6
7
8
9 (3) (a) Hiroto, S.; Miyake, Y.; Shinokubo, H. *Chem. Rev.* **2017**, *117*, 2910. (b) Beletskaya, I.
10
11 P.; Tyurin, V. S.; Uglov, A.; Stern, C.; Guillard, R. in *Handbook of Porphyrin Science, Vol. 37*
12
13 (Eds.: K. M. Kadish, K. M. Smith, R. Guillard), World Scientific Publishing, **2012**, p. 81.

14
15
16
17 (4) (a) Chumakov, D. E.; Khoroshutin, A. V.; Anisimov, A. V.; Kobrakov, K. I. *Chem.*
18
19 *Heterocycl. Comp.* **2009**, *45*, 259. (b) Wijesekera, T.; Dupré, D.; Cader, M. R.; Dolphin, D. *Bull.*
20
21 *Soc. Chim. Fr.* **1996**, *133*, 765.

22
23
24
25 (5) Hiroto, S.; Shinokubo, H. in *Handbook of Porphyrin Science*; Kadish, K. M., Smith, K. M.,
26
27 Guillard, R. Eds.; World Scientific: Singapore, **2016**; Vol. 26; p 233.

28
29
30
31 (6) (a) Bröring, M.; Köhler, S.; Kleeberg, C. *Angew. Chem. Int. Ed.* **2008**, *47*, 5658. (b) Ghosh,
32
33 A.; Wasbotten, I. H.; Davis, W.; Swarts, J. C. *Eur. J. Inorg. Chem.* **2005**, 4479.

34
35
36
37 (7) Ito, T.; Hayashi, Y.; Shimizu, S.; Shin, J.-Y.; Kobayashi, N.; Shinokubo, H. *Angew. Chem.*
38
39 *Int. Ed.* **2012**, *51*, 8542.

40
41
42 (8) (a) Nozawa, R.; Yamamoto, K.; Shin, J.-Y.; Hiroto, S.; Shinokubo, H. *Angew. Chem. Int.*
43
44 *Ed.* **2015**, *54*, 8454. (b) Fukuoka, T.; Uchida, K.; Sung, Y. M.; Shin, J.-Y.; Ishida, S.; Lim, J. M.;
45
46 Hiroto, S.; Furukawa, K.; Kim, D.; Iwamoto, T.; Shinokubo, H. *Angew. Chem. Int. Ed.* **2014**, *53*,
47
48 1506. (c) Shin, J.-Y.; Yamada, T.; Yoshikawa, H.; Awaga, K.; Shinokubo, H. *Angew. Chem. Int.*
49
50 *Ed.* **2014**, *53*, 3096. (d) Nozawa, R.; Tanaka, H.; Cha, W.-Y.; Hong, Y.; Hisaki, I.; Shimizu, S.;
51
52 Shin, J.-Y.; Kowalczyk, T.; Irle, S.; Kim, D.; Shinokubo, H. *Nat. Commun.* **2016**, *7*, 13620. (e)
53
54 Yoshida, T.; Shinokubo, H. *Mater. Chem. Front.* **2017**, *1*, 1853. (f) Yonezawa, T.; Shafie, S. A.;

1
2
3 Hiroto, S.; Shinokubo, H. *Angew. Chem. Int. Ed.* DOI: 10.1002/anie.201706134 and references
4
5 cited therein.
6
7

8
9 (9) (a) Deng, Z.; Li, X.; Stępień, M.; Chmielewski, P. J. *Chem.–Eur. J.* **2016**, *22*, 4231. (b) Liu,
10
11 B.; Li, X.; Stępień, M.; Chmielewski, P. J. *Chem.–Eur. J.* **2015**, *21*, 7790. (c) Liu, B.; Yoshida,
12
13 T.; Li, X.; Stępień, M.; Shinokubo, H.; Chmielewski, P. J. *Angew. Chem. Int. Ed.* **2016**, *55*,
14
15 13142. (d) Li, X.; Meng, Y.; Yi, P.; Stępień, M.; Chmielewski, P. J. *Angew. Chem. Int. Ed.* **2017**, *56*,
16
17 10810.
18
19

20
21 (10) Rousseau, G. in *Encyclopedia of Reagents for Organic Synthesis*; Paquette, L. A.; Crich,
22
23 D.; Fuchs, P. L.; Molander, G. A. Eds.; John Wiley & Sons, Ltd, **2001**. Vol. 2; p 895.
24
25

26
27 (11) (a) Becke, A. D. *Phys. Rev. A* **1988**, *38*, 3098. (b) Lee, C.; Yang, W.; Parr, R. G. *Phys.*
28
29 *Rev. B* **1988**, *37*, 785.
30
31

32
33 (12) Dolg, M.; Wedig, U.; Stoll, H.; Preuss, H. *J. Chem. Phys.* **1987**, *86*, 866.
34
35

36
37 (13) (a) Cancès, M. T.; Mennucci, B.; Tomasi, J. *J. Chem. Phys.* **1997**, *107*, 3032. (b) Cossi, M.
38
39 Barone, V.; Mennucci, B.; Tomasi, J. *Chem. Phys. Lett.* **1998**, *286*, 253. (c) Mennucci, B.;
40
41 Tomasi, J. *J. Chem. Phys.* **1997**, *106*, 5151. (d) Chipman, D. M. *J. Chem. Phys.* **2000**, *12*, 5558.
42
43

44 (14) Gaussian 09, Revision D.01, Frisch, M. J.; Trucks, G. W.; Schlegel, H. B.; Scuseria, G.
45
46 E.; Robb, M. A.; Cheeseman, J. R.; Scalmani, G.; Barone, V.; Mennucci, B.; Petersson, G. A.;
47
48 Nakatsuji, H.; Caricato, M.; Li, X.; Hratchian, H. P.; Izmaylov, A. F.; Bloino, J.; Zheng, G.;
49
50 Sonnenberg, J. L.; Hada, M.; Ehara, M.; Toyota, K.; Fukuda, R.; Hasegawa, J.; Ishida, M.;
51
52 Nakajima, T.; Honda, Y.; Kitao, O.; Nakai, H.; Vreven, T.; Montgomery, Jr., J. A.; Peralta, J. E.;
53
54 Ogliaro, F.; Bearpark, M.; Heyd, J. J.; Brothers, E.; Kudin, K. N.; Staroverov, V. N.; Kobayashi,
55
56
57
58
59
60

1
2
3 R.; Normand, J.; Raghavachari, K.; Rendell, A.; Burant, J. C.; Iyengar, S. S.; Tomasi, J.; Cossi,
4 M.; Rega, N.; Millam, J. M.; Klene, M.; Knox, J. E.; Cross, J. B.; Bakken, V.; Adamo, C.;
5 Jaramillo, J.; Gomperts, R.; Stratmann, R. E.; Yazyev, O.; Austin, A. J.; Cammi, R.; Pomelli, C.;
6 Ochterski, J. W.; Martin, R. L.; Morokuma, K.; Zakrzewski, V. G.; Voth, G. A.; Salvador, P.;
7
8 Dannenberg, J. J.; Dapprich, S.; Daniels, A. D.; Farkas, Ö.; Foresman, J. B.; Ortiz, J. V.;
9
10 Cioslowski, J.; Fox, D. J. Gaussian, Inc., Wallingford CT, **2009**.

11
12
13
14
15
16
17
18
19 (15) Software to optimize reaction paths along the user's expected ones, HPC Systems Inc.,
20
21 <http://www.hpc.co.jp/chem/react1.html>.

22
23
24 (16) (a) Jónsson, H.; Mills, G.; Jacobsen, K. W. in Classical and Quantum Dynamics in
25
26 Condensed Phase Simulations, (Eds.: B. J. Berne, G. Ciccotti, D. F. Coker), World Scientific
27
28 Publishing, **1998**, p. 385. (b) Henkelman, G.; Jónsson, H. *J. Chem. Phys.* **2000**, *113*, 9978.

32 33 34 35 36 37 38 39 40 41 42 43 44 45 46 47 48 49 50 51 52 53 54 55 56 57 58 59 60

SYNOPSIS

